The Plasminogen Receptor, Plg-R_KT, is Essential for Mammary Lobuloalveolar Development and Lactation

Lindsey A. Miles[1], **Nagyung Baik**[1], **Hongdong Bai**[2], **Helen P. Makarenkova**[1], **William B. Kiosses**[1], **Stan Krajewski**[3], **Francis J. Castellino**[4], **Alex Valenzuela**[5], **Nissi M. Varki**[5], **Barbara M. Mueller**[6], and **Robert J. Parmer**[2,7,*]

[1]Department of Molecular Medicine, The Scripps Research Institute, La Jolla, CA

[2]Veterans Administration San Diego Healthcare System, San Diego, CA

[3]Sanford-Burnham Medical Research Institute, La Jolla, CA

[4]W.M. Keck Center for Transgene Research, University of Notre Dame, Notre Dame, IN

[5]Department of Pathology, University of California San Diego, La Jolla, CA

[6]San Diego Biomedical Research Institute, San Diego, CA

[7]Department of Medicine, University of California San Diego, La Jolla, CA

Summary

Background—Lactational competence requires plasminogen, the zymogen of the serine protease, plasmin. Plg-R_KT is a unique transmembrane plasminogen receptor that promotes plasminogen activation to plasmin on cell surfaces. Plg-R_KT$^{-/-}$ mice are viable, but no offspring of Plg-R_KT$^{-/-}$ female mice survive to weaning.

Objectives—We investigated potential lactational failure in Plg-R_KT$^{-/-}$ mice and addressed causal mechanisms.

Methods—Fibrin accumulation, macrophage infiltration, processing of extracellular matrix components, effects of genetic deletion of fibrinogen, expression of fibrosis genes, and proliferation and apoptosis of epithelial cells were examined in lactating mammary glands of Plg-R_KT$^{-/-}$ and Plg-R_KT$^{+/+}$ mice.

Results—Milk was not present in the stomachs of offspring of Plg-R_KT$^{-/-}$ females and the pups were rescued by foster mothers. Although the mammary ductal tree developed normally in Plg-R_KT$^{-/-}$ glands, lobuloalveolar development was blocked by a hypertrophic fibrotic stroma and infiltrating macrophages were present. A massive accumulation of fibrin was also present in Plg-

$R_{KT}^{-/-}$ alveoli and ducts. Although this accumulation was decreased when Plg-$R_{KT}^{-/-}$ mice were made genetically heterozygous for fibrinogen, defects in lobuloalveolar development were not rescued by fibrinogen heterozygosity. Transcriptional profiling revealed that EGF was downregulated 12-fold in Plg-$R_{KT}^{-/-}$ glands. Furthermore, proliferation of epithelial cells was not detectable. In addition, the pro-survival protein, Mcl-1, was markedly downregulated and apoptosis was observed in Plg-$R_{KT}^{-/-}$ but not Plg-$R_{KT}^{+/+}$ glands.

Conclusions—Plg-R_{KT} is essential for lactogenesis and functions to maintain the appropriate stromal extracellular matrix environment, regulate epithelial cell proliferation and apoptosis, and, by regulating fibrinolysis, preserve alveolar and ductal patency.

Keywords

Fibrin; Fibrinolysis; Plasminogen; PLG-R(KT) protein; mouse; Receptors

Introduction

Post-embryonic mammary gland development to achieve lactational competence proceeds through distinct developmental stages: Branching morphogenesis when epithelium-lined ducts invade the mammary fat pad during puberty, development of lobular alveoli during pregnancy, differentiation of epithelial cells to enable milk secretion, and involution following weaning to restore the gland to the pre-pregnant state [1]. These steps are regulated by hormones, growth factors and proteinases expressed in a precise temporal pattern [2].

Lactational competence requires plasminogen [3, 4]. Plasminogen is activated to plasmin by locally secreted uPA or tPA. Plasmin is the major enzyme responsible for fibrin degradation [5, 6]. In addition, because plasmin is a broad spectrum serine protease, plasmin degrades other components of the extracellular matrix (ECM) including laminin and fibronectin [7, 8], processes prohormones [9–12] and activates pro-MMP's including MMP-3 [13]. Plasmin production also leads to MMP-9 activation through an intermediate enzyme that is activated by plasmin, potentially MMP-3 [13].

As a key mechanism for regulating plasmin activity, plasminogen binds specifically to cell surfaces and this interaction results in a marked increase in plasminogen activation on cells [reviewed in [14]]. Plasmin remains on the cell surface where it is protected from its major inhibitor, α_2-antiplasmin [14]. This leads to a local nidus of cell-associated broad spectrum proteolytic activity available to the cells for degradation of ECM components and activation of pro-MMP's and prohormones.

Plg-R_{KT} is a unique transmembrane plasminogen receptor that binds plasminogen via a C-terminal lysine exposed on the cell surface [15]. Plg-R_{KT} is highly colocalized with uPAR [15, 16] and promotes uPA-dependent plasminogen activation [17]. Plg-R_{KT} also binds tPA and promotes tPA-dependent plasminogen activation [15, 16]. Plg-R_{KT} is highly conserved with high interspecies homology and identity, no gaps in the sequences, and the presence of a C-terminal lysine for all 36 mammalian orthologs for which sequence information is available [15]. And Plg-R_{KT} is broadly expressed in human and murine tissues [18, 19].

We have recently developed and characterized mice deficient in Plg-R$_{KT}$ [20]. Plg-R$_{KT}$$^{-/-}$ mice are viable and fertile and survival of Plg-R$_{KT}$$^{-/-}$ mice and Plg-R$_{KT}$$^{+/+}$ littermates is not significantly different [20]. However, no offspring of Plg-R$_{KT}$$^{-/-}$ females survive to be weaned at 21 days [20]. Based on this observation and the established role of plasminogen in lactational competence [3, 4], here we investigate potential lactational failure in Plg-R$_{KT}$$^{-/-}$ mice and address mechanisms for this failure.

Materials and Methods

Mice and tissue treatment

Plg-R$_{KT}$ gene targeted mice [20] were backcrossed ten generations into the C57Bl/6J or 129XS/SVJ background. Unless otherwise indicated, mice in the C57Bl/6J background were used in this study. Fibrinogen deficient male mice [21] in the C57Bl/6J background were mated with Plg-R$_{KT}$$^{+/-}$ female mice and the resulting Plg-R$_{KT}$$^{+/-}$/Fgn$^{+/-}$ offspring were mated to obtain Plg-R$_{KT}$$^{-/-}$/Fgn$^{+/-}$ and Plg-R$_{KT}$$^{-/-}$/Fgn$^{-/-}$ mice and littermate controls.

Primiparous female mice (2–4 months) were used. For tissue harvesting, mice (2 days postpartum) were anesthetized with isoflurane and perfused intracardially with 20 ml ice cold phosphate buffered saline. For immunohistochemistry, abdominal mammary glands were either fixed in 4% paraformaldehyde for 18 hr at 4°C or frozen in OCT embedding medium. For DNA extraction, thoracic glands were snap frozen on dry ice. For protein extraction, thoracic mammary glands were harvested and lysed in Tissue Extraction Reagent I (Invitrogen) supplemented with protease inhibitor cocktail (Roche).

Antibodies and ELISA Kits

Primary antibodies used for western blot analysis were: anti-beta actin (LI-COR), anti-human fibrin(ogen) (Abcam), anti-casein (ABBIOTEC), anti-Mcl-1 and anti-cleaved caspase 3 (Cell Signaling Technology) and anti-entactin/nidogen (Millipore).

Primary antibodies used for immunohistochemical staining of paraffin embedded tissue were: anti-collagen IV and anti-α-smooth muscle actin (Abcam), anti-laminin 1 (R&D Systems), anti-mouse β_1 integrin (Chemicon), anti-mouse F4/80 (Biolegend),, anti-human fibrinogen (Dako), and anti-mouse Plg-R$_{KT}$, produced in our laboratory [15]. For immunohistochemistry of frozen sections, anti-Ser$_{28}$-phosphorylated histone H3 was from Sigma.

Mouse prolactin and uPA ELISA kits and an ELISA kit recognizing both fibrinogen and fibrin species were from Innovative Research, Inc. The mouse D-dimer ELISA kit was from LifeSpan Bioscience. The hydroxyproline assay kit was from Cell Biolabs.

Quantification of alveolar size, epithelial content and morphometry

Three photomicrographs at 400X in different areas were taken for each sample. Alveolar diameters were determined using the Keyence analyzer tools. Values for the three alveoli with the largest diameters in each sample were used for quantitative comparison between genotypes. Epithelial content in the same photomicrographs was quantified using the hybrid cell-count tool in the BZ-II Keyence Analyzer.

Keyence BZX700 software was used for quantitation of staining as described [22]. An average of 5, each, mouse segments of mammary glands per genotype were analyzed.

Expression profiling using the mouse fibrosis RT^2 array

RNA was obtained from fresh frozen thoracic mammary glands and reverse transcribed using the RT^2 First Strand Kit (SABiosciences, Qiagen). The Mouse Fibrosis PCR Array (PAMM-120Z; SABiosciences, Qiagen) was used to determine the expression levels of 84 individual genes important for dysregulated tissue remodeling.

Statistics

Data are as mean ± SEM. The statistical significance between groups was determined by ANOVA.

Study approval

All animal experiments were approved by the Institutional Animal Care and Use Committee of The Scripps Research Institute.

Results

Plg-R$_{KT}$ null mice cannot successfully lactate

Recently, we generated Plg-R$_{KT}$$^{-/-}$ mice using a homologous recombination technique, backcrossed them ten generations into the C57Bl/6J background, and evaluated spontaneous phenotypes. Plg-R$_{KT}$$^{-/-}$ females became pregnant and delivered live pups, but no offspring of Plg-R$_{KT}$$^{-/-}$ mothers survived to be weaned at 21 days [20]. To investigate the basis for death of offspring of Plg-R$_{KT}$$^{-/-}$ mice, here we have performed survival studies up to day 21 postpartum. Virgin Plg-R$_{KT}$$^{-/-}$ and Plg-R$_{KT}$$^{+/+}$ female mice (age 8 weeks) were mated to C57Bl/6J male mice (age 8 weeks). All offspring of Plg-R$_{KT}$$^{-/-}$ females died by postpartum day 2, with a median survival of one day (Fig. 1A). In contrast, 80% of the offspring of Plg-R$_{KT}$$^{+/+}$ females survived to be weaned at 21 days. The effect on pup survival was not strain-dependent. All pups (27/27) of Plg-R$_{KT}$$^{-/-}$ females backcrossed ten generations into the 129XS/SVJ background died within 2 days of birth, whereas 16/18 offspring (89%) of Plg-R$_{KT}$$^{+/+}$ females in the 129XS/SVJ background survived to weaning (χ^2=33.463, df=1, P<0.00000001).

We tested whether pup death was consistent with the inability of Plg-R$_{KT}$$^{-/-}$ mothers to successfully lactate. First, we observed pups for the presence of milk. No milk was observed in the stomachs of offspring of Plg-R$_{KT}$$^{-/-}$ mothers several hours after birth. In contrast, milk was readily apparent in the stomachs of offspring of Plg-R$_{KT}$$^{+/+}$ female mice. Second, offspring of Plg-R$_{KT}$$^{-/-}$ females were rescued by Balb/cBy foster mothers. The rescued mice survived past weaning and were healthy until sacrificed at 7–8.5 months. Thus, cross fostering demonstrated that the lactation defect was with the Plg-R$_{KT}$$^{-/-}$ mothers.

Blockade of lobuloalveolar development in Plg-R$_{KT}$ null mice

To further explore the basis for absence of lactational competence in the Plg-R$_{KT}$$^{-/-}$ mice we collected abdominal mammary tissue from primiparous Plg-R$_{KT}$$^{-/-}$ and Plg-R$_{KT}$$^{+/+}$ females

two days postpartum (lactation day 2). Abdominal mammary gland masses of Plg-R$_{KT}$$^{-/-}$ mice were significantly (50%) less than those of Plg-R$_{KT}$$^{+/+}$ mice (Fig. 1B). To assess milk production, mammary glands were lysed and western blotted with anti-casein and anti-actin as a loading control. The casein content of the Plg-R$_{KT}$$^{-/-}$ mammary glands was markedly less than that of Plg-R$_{KT}$$^{+/+}$ glands (Fig. 1C). We examined whether differences in milk production could be attributed to differences in prolactin levels because plasmin has the ability to process prohormones [9–12]. There were no significant differences in tissue prolactin levels in Plg-R$_{KT}$$^{+/+}$ and Plg-R$_{KT}$$^{-/-}$ female mice [8.6 ± 0.6 ng/mg of tissue and 8.9 ± 0.7 ng/mg of tissue, respectively (P=0.7894, n=4)].

The foregoing data suggested that Plg-R$_{KT}$ has a role in lactation. Therefore, we examined the localization of Plg-R$_{KT}$ within mammary glands using immunohistochemistry. Plg-R$_{KT}$ was prominently expressed on the apical surface of all luminal epithelial cells of Plg-R$_{KT}$$^{+/+}$ mice (Fig. 1D). In addition, weaker staining of the basal and lateral membranes of the luminal cells was observed. In controls, Plg-R$_{KT}$ immunoreactivity was not observed in Plg-R$_{KT}$$^{-/-}$ mammary tissue (Fig. 1E).

In order to understand the basis for decreased milk production by Plg-R$_{KT}$$^{-/-}$ mammary glands, histological analysis of abdominal mammary glands harvested two days postpartum was performed. H&E staining showed that the alveoli of Plg-R$_{KT}$$^{-/-}$ glands were strikingly smaller, atrophic and disordered while the ducts were distended (Fig. 2, B). Both alveoli and ducts showed accumulation of amorphous eosinophilic material, suggesting high protein content that was not observed in Plg-R$_{KT}$$^{+/+}$ glands (Fig. 2, compare A and B). Compared with Plg-R$_{KT}$$^{+/+}$ glands (Fig. 2C), whole mount preparations also showed decreased alveolar size and number in Plg-R$_{KT}$$^{-/-}$ glands (Fig. 2D). Furthermore, alveolar diameter was markedly decreased in Plg-R$_{KT}$$^{-/-}$ glands compared to glands of Plg-R$_{KT}$$^{+/+}$ littermates (Fig. 2E). And per cent epithelial content, reflecting the number of alveoli, was markedly decreased in Plg-R$_{KT}$$^{-/-}$ glands (Fig. 2F).

Plg-R$_{KT}$ deficiency does not affect branching morphogenesis during puberty

Development of the ductal tree in wild type mice takes place from birth to sexual maturity. In order to examine the effect of Plg-R$_{KT}$ deletion on this process, abdominal mammary glands harvested from virgin mice at 5, 8, 12 and 16 weeks of age were examined. Whole mount preparations showed no significant differences in ductal length or the number of terminal end buds. In addition, examination of H&E stained paraffin sections showed that ductal density and orientation of the surrounding connective tissue were similar in Plg-R$_{KT}$$^{-/-}$ and Plg-R$_{KT}$$^{+/+}$ glands (data not shown).

Plg-R$_{KT}$ deficiency does not affect basement membrane deposition nor disrupt the myo-epithelial cell layer of mammary glands

Immunohistochemical comparison of basement membranes showed the normal presence and location of collagen IV and laminin in both Plg-R$_{KT}$$^{-/-}$ and Plg-R$_{KT}$$^{+/+}$ mammary glands (Fig. 3, compare A and B and compare C and D, respectively). Furthermore, Plg-R$_{KT}$ deletion did not affect the integrity of the myoepithelial cell layer, as shown by staining with anti-smooth muscle actin (Fig. 3, compare E and F). (By morphometric analysis,

immunostaining for smooth muscle actin was decreased by 0.3-fold, consistent with the reduced number of alveoli.) And, although the Plg-R$_{KT}$$^{-/-}$ alveoli were smaller than those of Plg-R$_{KT}$$^{+/+}$ littermates the orientation of the epithelial cells appeared normal as revealed by staining with anti-β$_1$-integrin (Fig. 3, compare G and H). However, in Plg-R$_{KT}$$^{-/-}$ glands, there was a marked enhancement of collagen, laminin and β$_1$-integrin signals (1.7-fold, 7.0-fold and 1.9-fold, respectively, by morphometric analyses) within the stroma in an actively remodeled adipose tissue, apparently compensating for the loss of alveolar structures.

Plg-R$_{KT}$ deletion alters the ECM in lactating mammary glands

Survival and lactogenesis require the appropriate extracellular environment [23–25]. We evaluated ECM components of Plg-R$_{KT}$$^{+/+}$ and Plg-R$_{KT}$$^{-/-}$ abdominal mammary glands collected at lactation day 2. Excessive collagen deposition (1.9-fold increase by morphometric analysis) was observed within the mammary adipose tissue surrounding the alveoli of the Plg-R$_{KT}$$^{-/-}$ mammary glands and fibrosis was also present within the surrounding adipose tissue of the Plg-R$_{KT}$$^{-/-}$ mammary glands, as assessed by trichrome staining (Fig. 4, compare A and B). Correspondingly, when collagen content was assessed in a hydroxyproline assay, the hydroxyproline contents were 14.9 ±2.9 ng/mg and 6.2 ±0.5 ng/mg of mammary tissue for Plg-R$_{KT}$$^{-/-}$ and Plg-R$_{KT}$$^{+/+}$ littermates, respectively (P= 0.011, n=6–8). Consistent with the fibrotic ECM, cellular infiltrates were also observed in the trichrome-stained tissue from Plg-R$_{KT}$$^{-/-}$ glands (Fig. 4B, arrows). Specific staining for macrophages with anti-F4/80 mAb revealed marked accumulation of macrophages (4.4-fold increase by morphometric analysis), relative to the glands of Plg-R$_{KT}$$^{+/+}$ littermates (Fig. 4, compare C and D). Because Plg-R$_{KT}$ binds plasminogen and promotes plasminogen activation [14] and fibrin deposition takes place in plasminogen deficient (Plg$^{-/-}$) mammary glands [4], we also stained the tissue for the presence of fibrin. Fibrin was detected in Plg-R$_{KT}$$^{+/+}$ glands, consistent with its function as a scaffolding protein. In contrast, Plg-R$_{KT}$$^{-/-}$ glands showed excessive fibrin deposition (1.5-fold increase by morphometric analysis) within the distended alveoli and also in the fibrotic mammary adipose tissue surrounding the alveoli (Fig. 4, compare E and F). Both fibrinogen [4] and plasminogen [26, 27], as well as uPA and tPA [28] are components of breast milk. In addition, the content of the ECM component, entactin/nidogen, was significantly increased in Plg-R$_{KT}$$^{-/-}$ glands (Fig. 5, A,B).

Western blot analysis demonstrated increased fibrin content in Plg-R$_{KT}$$^{-/-}$ glands (Fig. 5C). And the fibrin(ogen) content of mammary tissue determined by quantitative western blotting (Fig. 5D) and ELISA (that recognizes both fibrinogen and fibrin species) was significantly greater in Plg-R$_{KT}$$^{-/-}$ glands (Fig. 5.E). Plasma D-dimer levels did not differ between genotypes, suggesting a local, but not systemic, effect of Plg-R$_{KT}$ deletion on fibrinolysis [8.64 ± 0.46 pg/ml and 10.08 ± 1.97 pg/ml for Plg-R$_{KT}$$^{+/+}$ and Plg-R$_{KT}$$^{-/-}$ plasma, respectively (P=0.4927, n=6)].

We tested whether genotype-dependent differences in mammary tissue uPA concentrations might account for differences in fibrin clearance. uPA levels were not significantly different between the genotypes: 4.5±0.81 ng/mg and 5.5 ± 0.77 ng/mg of mammary tissue protein in Plg-R$_{KT}$$^{+/+}$ and Plg-R$_{KT}$$^{-/-}$ glands, respectively (P=0.386, n=4).

Effect of Fibrinogen Deletion on Lactation by Plg-R$_{KT}$$^{-/-}$ Mice

Because we had observed fibrin deposition within the alveoli and reduction of fibrinogen levels to 50% allows Plg$^{-/-}$ mice to lactate without problems [4], we tested whether deficiency of fibrinogen would rescue breast development. We generated Plg-R$_{KT}$$^{-/-}$/Fgn$^{-/-}$ mice and mated them with wild type C57Bl/6J male mice. Similarly to what is observed with Fgn$^{-/-}$ mice [21, 29] all pregnant Plg-R$_{KT}$$^{-/-}$/Fgn$^{-/-}$ females died by day 9 of gestation due to uterine bleeding. In contrast, Plg-R$_{KT}$$^{-/-}$/Fgn$^{+/-}$ mice survived pregnancy and were able to give birth successfully. Therefore, we examined lactational competence in Plg-R$_{KT}$$^{-/-}$/Fgn$^{+/-}$ mice. [Fibrinogen plasma levels were 1.4 ± 0.1 mg/ml in mice genetically wild type for fibrinogen and 0.7 ± 0.1 mg/ml for mice genetically heterozygous for fibrinogen (P=0.0016, n = 5)]. Fibrinogen heterozygosity did not rescue survival of offspring of Plg-R$_{KT}$$^{-/-}$ females. All offspring (34/34) of Plg-R$_{KT}$$^{-/-}$/Fgn$^{+/-}$ females died by postpartum day 2, whereas 25/26 offspring (96%) of Plg-R$_{KT}$$^{+/+}$/Fgn$^{+/+}$ females survived to weaning (χ^2=52.158, df=1, P< 0.001) (Fig. 6A).

Abdominal mammary gland masses of Plg-R$_{KT}$$^{-/-}$/Fgn$^{+/-}$ mice were significantly (45%) less than those of Plg-R$_{KT}$$^{+/+}$/Fgn$^{+/-}$ mice (Fig. 6B). [Body weights of Plg-R$_{KT}$$^{-/-}$/Fgn$^{+/-}$ and Plg-R$_{KT}$$^{-/-}$/Fgn$^{+/+}$ mice were not significantly different. However, Plg-R$_{KT}$ deletion did have an effect on body weight in both the fibrinogen wild type and heterozygous backgrounds (Supplemental Fig. S1), consistent with our previous report showing a significant effect of Plg-R$_{KT}$ deletion on body weights of female mice [20]]. H&E staining showed decreased alveolar diameter and number of alveoli in Plg-R$_{KT}$$^{-/-}$/Fgn$^{+/-}$ glands (Fig. 6D) compared with glands of Plg-R$_{KT}$$^{+/+}$/Fgn$^{+/-}$ littermates (Fig. 6C). Mean alveolar diameters of Plg-R$_{KT}$$^{-/-}$/Fgn$^{+/-}$ glands were markedly less than those of Plg-R$_{KT}$$^{+/+}$/Fgn$^{+/-}$ littermates (Fig. 6E). The per cent epithelial content of Plg-R$_{KT}$$^{-/-}$/Fgn$^{+/-}$ glands was also markedly less than that of Plg-R$_{KT}$$^{+/+}$/Fgn$^{+/-}$ littermates (Fig. 6F). Interestingly, deletion of Plg-R$_{KT}$ on the heterozygous fibrinogen background significantly decreased epithelial content compared with Plg-R$_{KT}$ deletion on the fibrinogen wild type background, while an effect of fibrinogen heterozygosity was not observed in Plg-R$_{KT}$$^{+/+}$ glands (Fig. 6F). When Plg-R$_{KT}$$^{-/-}$/Fgn$^{+/-}$ glands were immunostained for fibrin(ogen) excessive fibrin deposition was observed in the stroma surrounding the mammary adipose tissue (Fig. 6H, curved arrow) and surrounding the alveoli (Fig. 6H, straight arrow) compared with glands of Plg-R$_{KT}$$^{+/+}$/Fgn$^{+/-}$ littermates (Fig. 6G). Although secretions were observed in alveoli and ducts of Plg-R$_{KT}$$^{-/-}$/Fgn$^{+/-}$ glands, fibrin deposition was not observed in these structures (Fig. 6H), in contrast to the excessive fibrin deposition observed in Plg-R$_{KT}$$^{-/-}$/Fgn$^{+/+}$ glands (Fig. 4F).

We investigated the effect of fibrinogen deletion on epithelial content further by quantifying the per cent total mammary area occupied by epithelia in tissue harvested from fibrinogen null mice at day 8 of pregnancy (before their spontaneous death). At this developmental time point, there was no significant effect of Plg-R$_{KT}$ genotype on either gland weight or epithelial content (Supplemental Fig. S2). However, deletion of Plg-R$_{KT}$ on the fibrinogen null background significantly decreased mammary epithelial content, consistent with a role for a fibrin scaffold at this stage of lactogenesis.

Fibrosis Expression Signatures are Distinct in Lactating Plg-R$_{KT}$$^{-/-}$ and Plg-R$_{KT}$$^{+/+}$ Mammary Glands

Because deficient fibrin degradation could not fully account for the lactation defect in Plg-R$_{KT}$$^{-/-}$ mice and because a fibrotic stroma was observed in Plg-R$_{KT}$$^{-/-}$ glands (Fig. 4, A and B), we used fibrosis gene transcription profiling to investigate differences in gene expression profiles of Plg-R$_{KT}$$^{-/-}$ and Plg-R$_{KT}$$^{+/+}$ mammary glands harvested two days postpartum. Expression of 84 genes was analyzed and fold changes are shown in Supplementary Table 1. We identified 25 genes for which expression in Plg-R$_{KT}$$^{-/-}$ glands was significantly ($P <$ 0.05) different than in Plg-R$_{KT}$$^{+/+}$ glands by a factor of >2-fold. Twenty-one genes were upregulated and 4 were down-regulated (Table 1). Upregulation of remodeling enzymes and inhibitors (Mmp2, Mmp9 and Timp2), inflammatory cytokines and chemokines (Il1a, Il4 and TNF) and integrins (α2, β1, β3, β6, and β8) within the mammary tissue was consistent with the marked infiltration of macrophages observed in Plg-R$_{KT}$$^{-/-}$ glands (Fig. 4D). In addition, TGFβ3 and its targets, Smad 2 and CTGF (connective tissue growth factor or CCN2) were strikingly upregulated. CTGF promotes matrix protein deposition and fibrogenesis [30], which is consistent with the phenotype of the Plg-R$_{KT}$$^{-/-}$ glands. In addition, Mmp1a was markedly downregulated while Timp2 was markedly upregulated in Plg-R$_{KT}$$^{-/-}$ glands, consistent with extensive collagen deposition in this genotype.

Plg-R$_{KT}$ Deletion Decreases Epithelial Cell Proliferation and Increases Epithelial Cell Apoptosis

Of the genes downregulated in Plg-R$_{KT}$$^{-/-}$ glands, EGF was the most extensively downregulated gene identified (12-fold-less expression) (Table 1). EGF protein levels were 21.2 ±1.2 and 42.3 ± 3.7 pg/mg of tissue for Plg-R$_{KT}$$^{-/-}$ and Plg-R$_{KT}$$^{+/+}$ glands, respectively, P=0.0003, n=6), as determined by ELISA. Therefore, we examined the glands for proliferation by staining with antibodies against Ser$_{28}$-phosphorylated histone H3 (a marker of cell proliferation). Proliferating epithelial cells were abundant in Plg-R$_{KT}$$^{+/+}$ glands, but proliferation was not detectable in Plg-R$_{KT}$$^{-/-}$ glands (Fig. 7A).

EGF orchestrates increased translation of the pro-survival Bcl-2 family protein, Mcl-1, and genetic deletion of Mcl-1 results in increased epithelial apoptosis, defective alveolar development in mouse mammary glands, and death of all offspring by 2 days postpartum [31]. In western blotting Mcl-1 expression was observed in Plg-R$_{KT}$$^{+/+}$ glands, but was not detectable in Plg-R$_{KT}$$^{-/-}$ glands (Fig. 7B), while the cleaved (activated) caspase-3 doublet was present in Plg-R$_{KT}$$^{-/-}$ glands, but was not detectable in Plg-R$_{KT}$$^{+/+}$ glands (Fig. 7C).

DISCUSSION

Our results demonstrate and provide mechanistic insight for the complete failure of lactation in Plg-R$_{KT}$$^{-/-}$ mice. We found that deletion of Plg-R$_{KT}$$^{-/-}$ exerted a selective effect on lobuloalveolar development. The effect of Plg-R$_{KT}$ deletion on alveologenesis was severe, with markedly decreased alveolar diameter and alveolar number in Plg-R$_{KT}$$^{-/-}$ glands. Milk production was severely and significantly decreased in Plg-R$_{KT}$$^{-/-}$ mammary glands.

Successful lactogenesis requires the appropriate extracellular environment [23–25]. An abnormal fibrotic ECM was observed in the stroma of Plg-R$_{KT}$$^{-/-}$ glands. The content of entactin/nidogen-1 was significantly increased and increased collagen deposition was observed in the connective tissue and adipose tissue surrounding the alveoli. Notably, despite the extensive collagen deposition, expression of collagen type Iα2 and collagen type IIIα1 genes were not significantly up-regulated, suggesting that the increased collagen deposition was consistent with impaired collagen remodeling.

In additional evidence for abnormal proteolysis in Plg-R$_{KT}$$^{-/-}$ glands, excessive fibrin deposition was present on the stroma and on adipocytes surrounding the alveoli. Marked fibrin deposition was also noteworthy within the distended alveoli and entactic ducts of Plg-R$_{KT}$$^{-/-}$ mammary glands. Milk contains both plasminogen [26, 27] and fibrinogen [4] as well as uPA and tPA [28] and it has been suggested that plasmin(ogen) in milk serves to degrade fibrin to maintain alveolar and ductal patency [27]. Notably fibrin deposition is also observed in Plg$^{-/-}$ glands at postpartum day 2 [4]. Our results suggest that Plg-R$_{KT}$ on the surface of epithelial cells may be essential for maintenance of alveolar and ductal patency by promoting plasminogen activation. Our current results provide the first example of a requirement for Plg-R$_{KT}$ for efficient fibrinolysis *in vivo*. In an extensive tissue survey of Plg-R$_{KT}$$^{-/-}$ mice, we did not detect spontaneous fibrin deposition [20]. Thus, the challenge of pregnancy and lactation in Plg-R$_{KT}$$^{-/-}$ mice unmasked this key *in vivo* role of Plg-R$_{KT}$.

The presence of the fibrotic ECM is consistent with deficient proteolysis within the mammary gland and with the increased expression of CTGF. The fibrotic phenotype observed in Plg-R$_{KT}$$^{-/-}$ glands did not appear to be due to differences in myoblast infiltration and proliferation because expression of smooth muscle actin (a myoblast marker) was not different in Plg-R$_{KT}$$^{+/+}$ and Plg-R$_{KT}$$^{-/-}$ mammary glands (Supplementary Table 1). Consistent with the presence of excessive fibrin and collagen, numerous macrophage infiltrates were observed in Plg-R$_{KT}$$^{-/-}$ glands that were not detected in Plg-R$_{KT}$$^{+/+}$ tissue. The increased cellular infiltrate is noteworthy in view of the requirement for Plg-R$_{KT}$ for macrophage recruitment in experimental peritonitis [17, 20]. Notably, similar cellular infiltrates are observed in spontaneously thrombotic organs of Plg$^{-/-}$ mice [5, 6] although Plg$^{-/-}$ mice also exhibit defective macrophage recruitment in experimental peritonitis [32]. These differences may relate to differential expression of Plg-R$_{KT}$ on different monocyte subsets [33] and/or to differences in the expression and contribution of other plasminogen receptors on infiltrating macrophages.

Despite similarities in fibrin deposition in Plg-R$_{KT}$$^{-/-}$ and Plg$^{-/-}$ glands, the severity and histological basis of the lactation defect in Plg-R$_{KT}$$^{-/-}$ mice was much more pronounced than that of Plg$^{-/-}$ mice [3, 4]. Notably, reduction of fibrinogen levels to 50% allows Plg$^{-/-}$ mice to lactate without problems [4]. In contrast, reduction of fibrinogen levels to 50% in Plg-R$_{KT}$$^{-/-}$ mice did not rescue the defective lactation phenotype. Thus, although blockade of ducts with fibrin may play a role, it cannot account for the complete failure of lactation and impaired alveologenesis in Plg-R$_{KT}$$^{-/-}$ mice. Thus, in addition to impaired fibrinolysis, plasminogen-independent functions of Plg-R$_{KT}$ may contribute to the defective lactation phenotype.

Using fibrosis gene transcription profiling, EGF was the most extensively downregulated gene identified at lactation day 2 (12-fold-less expression in Plg-R$_{KT}^{-/-}$ compared with Plg-R$_{KT}^{+/+}$ glands). Successful lactation requires the function of a family of growth factors, exerting activities at the different stages of mammary development [2]. EGF is the most abundant of all differentially expressed cytokines and growth factors in luminal cells of lactating glands (>100-fold increase between late pregnancy and lactation) [31]. And, of ligands for the EGF receptor (EGFR), EGF is exclusively induced at lactation [31]. Notably, mice homozygous for a mutant EGFR that does not bind EGF exhibit a reduction in size of mammary ducts and lobules and a partial lactation defect [34]. Markedly deficient epithelial proliferative capacity, resulting in blockade of lobuloalveolar development of Plg-R$_{KT}^{-/-}$ glands, is consistent with downregulation of EGF.

EGF orchestrates increased translation of the pro-survival Bcl-2 family protein, Mcl-1, and genetic deletion of Mcl-1 in mice results in increased epithelial apoptosis, defective alveolar development and death of all offspring by 2 days postpartum [31]. Mcl-1 expression was observed in Plg-R$_{KT}^{+/+}$ glands, but was not detectable in Plg-R$_{KT}^{-/-}$ glands. Down-regulation of Mcl-1 translation may, therefore, contribute to the increase in apoptosis observed in Plg-R$_{KT}^{-/-}$ glands.

The effect of Plg-R$_{KT}$ deletion on EGF biosynthesis is likely to be independent of plasmin(ogen) as we found no significant effect of plasminogen deletion on EGF levels in lactating mammary glands (60.8 ±12.0 and 47.0 ± 2.4 pg/mg for Plg$^{-/-}$ and Plg $^{+/+}$ glands, respectively, P=0.283, n=6). Correspondingly, Plg$^{-/-}$ glands do not exhibit defective proliferative ability nor defects in lobuloalveolar development [3, 4]. Thus, the severe structural alterations observed in Plg-R$_{KT}^{-/-}$ glands can most likely be ascribed to a failure of EGF/Mcl-1 signaling. Plg-R$_{KT,}$ either alone or in complex with other transmembrane proteins may transmit signals from ligands yet to be identified that modulate EGF expression.

In summary, our results suggest that, Plg-R$_{KT}$ has multiple functions in lactogenesis. Plg-R$_{KT}$ promotes maintenance of the appropriate extracellular environment supporting epithelial development. Plg-R$_{KT}$ regulates the balance of epithelial proliferation and apoptosis. And Plg-R$_{KT}$ is a key regulator of fibrin surveillance within the alveoli. Thus, Plg-R$_{KT}$ is required for survival of the species, based on the total failure of lactation in Plg-R$_{KT}^{-/-}$ mice.

These studies also have major implications for the function of other organs that undergo post-embryonic morphogenesis including kidney [35], prostate [36], lacrimal gland [37], and salivary gland [38] in that Plg-R$_{KT}$ may regulate morphogenesis, particularly epitheliogenesis, during responses of these organs to pathological insults.

Supplementary Material

Refer to Web version on PubMed Central for supplementary material.

Acknowledgments

Reference List

1. Hinck L, Silberstein GB. Key stages in mammary gland development: the mammary end bud as a motile organ. Breast Cancer Res. 2005; 7:245–51. DOI: 10.1186/bcr1331 [PubMed: 16280048]

2. Hovey RC, Trott JF, Vonderhaar BK. Establishing a framework for the functional mammary gland: from endocrinology to morphology. J Mammary Gland Biol Neoplasia. 2002; 7:17–38. [PubMed: 12160083]

3. Lund LR, Bjorn SF, Sternlicht MD, Nielsen BS, Solberg H, Usher PA, Osterby R, Christensen IJ, Stephens RW, Bugge TH, Dano K, Werb Z. Lactational competence and involution of the mouse mammary gland require plasminogen. Development. 2000; 127:4481–92. [PubMed: 11003846]

4. Green KA, Nielsen BS, Castellino FJ, Romer J, Lund LR. Lack of plasminogen leads to milk stasis and premature mammary gland involution during lactation. Dev Biol. 2006; 299:164–75. [PubMed: 16949567]

5. Bugge TH, Flick MJ, Daugherty CC, Degen JL. Plasminogen deficiency causes severe thrombosis but is compatible with development and reproducton. Genes Dev. 1995; 9:794–807. [PubMed: 7705657]

6. Ploplis VA, Carmeliet P, Vazirzadeh S, Van VI, Moons L, Plow EF, Collen D. Effects of disruption of the plasminogen gene on thrombosis, growth, and health in mice. Circulation. 1995; 92:2585–93. [PubMed: 7586361]

7. Liotta LA, Goldfarb RH, Brundage R, Siegal GP, Terranova V, Garbisa S. Effect of plasminogen activator (urokinase), plasmin, and thrombin on glycoprotein and collagenous components of basement membrane. Cancer Res. 1981; 41:4629–36. [PubMed: 6458354]

8. Liotta LA, Goldfarb RH, Terranova VP. Cleavage of laminin by thrombin and plasmin: Alpha thrombin selectively cleaves the beta chain of laminin. Thromb Res. 1981; 21:663–73. [PubMed: 6455777]

9. Hoover-Plow J, Wang N, Ploplis VA. Growth and behavioral development in plasminogen gene-targeted mice. Growth, Development and Aging. 1999; 63:13–32.

10. Parmer RJ, Mahata M, Gong Y, Mahata S, Jiang Q, O'Connor DT, Xi X-P, Miles LA. Processing of chromogranin A by plasmin provides a novel mechanism for regulating catecholamine secretion. J Clin Invest. 2000; 106:907–15. [PubMed: 11018079]

11. Jiang Q, Taupenot L, Mahata SK, Mahata M, O'Connor DT, Miles LA, Parmer RJ. Proteolytic cleavage of chromogranin A (CgA) by plasmin. Selective liberation of a specific bioactive CgA fragment that regulates catecholamine release. J Biol Chem. 2001; 276:25022–9. DOI: 10.1074/jbc.M101545200 [PubMed: 11342539]

12. Wang N, Zhang L, Miles L, Hoover-Plow J. Plasminogen regulates pro-opiomelanocortin processing. J Thromb Haemost. 2004; 2:785–96. [PubMed: 15099286]

13. Ramos-DeSimone N, Hahn-Dantona E, Sipley J, Nagase H, French DL, Quigley JP. Activation of matrix metalloproteinase-9 (MMP-9) via a converging plasmin/stromelysin-1 cascade enhances tumor cell invasion. J Biol Chem. 1999; 274:13066–76. [PubMed: 10224058]

14. Miles LA, Parmer RJ. Plasminogen receptors: the first quarter century. Semin Thromb Hemost. 2013; 39:329–37. [PubMed: 23532575]

15. Andronicos NM, Chen EI, Baik N, Bai H, Parmer CM, Kiosses WB, Kamps MP, Yates JR III, Parmer RJ, Miles LA. Proteomics-based discovery of a novel, structurally unique, and developmentally regulated plasminogen receptor, Plg-RKT, a major regulator of cell surface plasminogen activation. Blood. 2010; 115:1319–30. [PubMed: 19897580]

16. Bai H, Baik N, Kiosses WB, Krajewski S, Miles LA, Parmer RJ. The novel plasminogen receptor, plasminogen receptor(KT) (Plg-R(KT)), regulates catecholamine release. J Biol Chem. 2011; 286:33125–33. [PubMed: 21795689]

17. Lighvani S, Baik N, Diggs JE, Khaldoyanidi S, Parmer RJ, Miles LA. Regulation of macrophage migration by a novel plasminogen receptor Plg-RKT. Blood. 2011; 118:5622–30. [PubMed: 21940822]

18. Su AI, Cooke MP, Ching KA, Hakak Y, Walker JR, Wiltshire T, Orth AP, Vega RG, Sapinoso LM, Moqrich A, Patapoutian A, Hampton GM, Schultz PG, Hogenesch JB. Large-scale analysis of the human and mouse transcriptomes. Proc Natl Acad Sci U S A. 2002; 99:4465–70. [PubMed: 11904358]

19. Su AI, Wiltshire T, Batalov S, Lapp H, Ching KA, Block D, Zhang J, Soden R, Hayakawa M, Kreiman G, Cooke MP, Walker JR, Hogenesch JB. A gene atlas of the mouse and human protein-encoding transcriptomes. Proc Natl Acad Sci U S A. 2004; 101:6062–7. [PubMed: 15075390]

20. Miles LA, Baik N, Lighvani S, Khaldoyanidi S, Varki NM, Bai H, Mueller BM, Parmer RJ. Deficiency of plasminogen receptor, Plg-RKT, causes defects in plasminogen binding and inflammatory macrophage recruitment in vivo. J Thromb Haemost. 2017; 15:155–62. DOI: 10.1111/jth.13532 [PubMed: 27714956]

21. Iwaki T, Sandoval-Cooper MJ, Paiva M, Kobayashi T, Ploplis VA, Castellino FJ. Fibrinogen stabilizes placental-maternal attachment during embryonic development in the mouse. Am J Pathol. 2002; 160:1021–34. [PubMed: 11891199]

22. Zhou Q, Kiosses WB, Liu J, Schimmel P. Tumor endothelial cell tube formation model for determining anti-angiogenic activity of a tRNA synthetase cytokine. Methods. 2008; 44:190–5. [PubMed: 18241800]

23. Streuli CH, Bailey N, Bissell MJ. Control of mammary epithelial differentiation: basement membrane induces tissue-specific gene expression in the absence of cell-cell interaction and morphological polarity. J Cell Biol. 1991; 115:1383–95. [PubMed: 1955479]

24. Boudreau N, Sympson CJ, Werb Z, Bissell MJ. Suppression of ICE and apoptosis in mammary epithelial cells by extracellular matrix. Science. 1995; 267:891–3. [PubMed: 7531366]

25. Pullan S, Wilson J, Metcalfe A, Edwards GM, Goberdhan N, Tilly J, Hickman JA, Dive C, Streuli CH. Requirement of basement membrane for the suppression of programmed cell death in mammary epithelium. J Cell Sci. 1996; 109(Pt 3):631–42. [PubMed: 8907708]

26. Greenberg R, Groves ML. Plasmin cleaves human beta-casein. Biochem Biophys Res Commun. 1984; 125:463–8. [PubMed: 6240266]

27. Heegaard CW, Larsen LB, Rasmussen LK, Hojberg KE, Petersen TE, Andreasen PA. Plasminogen activation system in human milk. J Pediatr Gastroenterol Nutr. 1997; 25:159–66. [PubMed: 9252902]

28. Politis I, White JH, O'Hare K, Zavizion B, Gilmore J, Caler W. Distribution of plasminogen activator forms in fractions of goat milk. J Dairy Sci. 1994; 77:2900–6. [PubMed: 7836578]

29. Suh TT, Holmback K, Jensen NJ, Daugherty CC, Small K, Simon DI, Potter S, Degen JL. Resolution of spontaneous bleeding events but failure of pregnancy in fibrinogen-deficient mice. Genes Dev. 1995; 9:2020–33. [PubMed: 7649481]

30. Jun JI, Lau LF. Taking aim at the extracellular matrix: CCN proteins as emerging therapeutic targets. Nat Rev Drug Discov. 2011; 10:945–63. [PubMed: 22129992]

31. Fu NY, Rios AC, Pal B, Soetanto R, Lun AT, Liu K, Beck T, Best SA, Vaillant F, Bouillet P, Strasser A, Preiss T, Smyth GK, Lindeman GJ, Visvader JE. EGF-mediated induction of Mcl-1 at the switch to lactation is essential for alveolar cell survival. Nat Cell Biol. 2015; 17:365–75.1. [PubMed: 25730472]

32. Ploplis VA, French EL, Carmeliet P, Collen D, Plow EF. Plasminogen deficiency differentially affects recruitment of inflammatory cell populations in mice. Blood. 1998; 91:2005–9. [PubMed: 9490683]

33. Thaler, B., Hohensinner, PJ., Baumgartner, J., Baik, N., Krychtiuk, KA., Maurer, G., Huber, K., Speidl, WS., Parmer, RJ., Miles, LA., Wojta, J. Differential Expression of the Plasminogen Receptor Plg-RKT in Monocyte and Macrophage Subsets - Possible Functional Consequences in

Atherogenesis. Presented at the 1st Joint Meeting of ISFP and PA Workshop in Shizuoka; Japan. Oct, 2016;

34. Fowler KJ, Walker F, Alexander W, Hibbs ML, Nice EC, Bohmer RM, Mann GB, Thumwood C, Maglitto R, Danks JA, et al. A mutation in the epidermal growth factor receptor in waved-2 mice has a profound effect on receptor biochemistry that results in impaired lactation. Proc Natl Acad Sci U S A. 1995; 92:1465–9. [PubMed: 7533293]

35. Shah MM, Sampogna RV, Sakurai H, Bush KT, Nigam SK. Branching morphogenesis and kidney disease. Development. 2004; 131:1449–62. [PubMed: 15023929]

36. Thomson AA, Marker PC. Branching morphogenesis in the prostate gland and seminal vesicles. Differentiation. 2006; 74:382–92. [PubMed: 16916376]

37. Gromova A, Voronov DA, Yoshida M, Thotakura S, Meech R, Dartt DA, Makarenkova HP. Lacrimal Gland Repair Using Progenitor Cells. Stem cells translational medicine. 2017; 6:88–98. [PubMed: 28170196]

38. Patel VN, Rebustini IT, Hoffman MP. Salivary gland branching morphogenesis. Differentiation. 2006; 74:349–64. [PubMed: 16916374]

39. Versteeg HH, Schaffner F, Kerver M, Ellies LG, Andrade-Gordon P, Mueller BM, Ruf W. Protease-activated receptor (PAR) 2, but not PAR1, signaling promotes the development of mammary adenocarcinoma in polyoma middle T mice. Cancer Res. 2008; 68:7219–27. [PubMed: 18757438]

Essentials

- Plg-R$_{KT}$$^{-/-}$ female mice give birth, but no offspring of Plg-R$_{KT}$$^{-/-}$ female mice survive to weaning.

- Causal mechanisms of potential lactational failure in Plg-R$_{KT}$$^{-/-}$ mice are unknown.

- Plg-R$_{KT}$ regulates extracellular matrix remodeling, cell proliferation, apoptosis, fibrin surveillance.

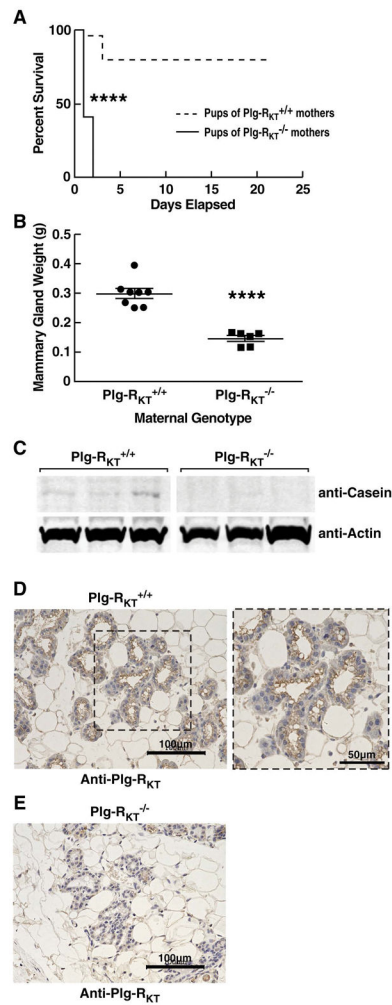- Plg-R$_{KT}$ is essential for lactogenesis and mammary lobuloalveolar development.

Figure 1. Plg-R$_{KT}$ null mice cannot successfully lactate

(A), Survival data are shown for a cohort of offspring of Plg-R$_{KT}^{+/+}$ (dashed lines) and Plg-R$_{KT}^{-/-}$ (solid lines) primiparous female littermates: 48 offspring of Plg-R$_{KT}^{+/+}$ mice and 30 offspring of Plg-R$_{KT}^{-/-}$ mice. **** P<0.0001 Log-rank (Mantel Cox) test]. **(B),** Abdominal mammary glands were collected 2 days postpartum from primiparous Plg-R$_{KT}^{+/+}$ and Plg-R$_{KT}^{-/-}$ female littermates and weighed. **** P<0.0001, n=6 Plg-R$_{KT}^{-/-}$ mice and n=8 Plg-R$_{KT}$ mice$^{+/+}$ **(C),** Thoracic mammary glands (harvested 2 days postpartum) were lysed and western blotted with anti-casein and with anti-actin, as a loading control. When using anti-casein antibody, membranes were blocked with LI-COR Casein blocking Buffer. **(D,E),** Abdominal mammary glands were collected 2 days postpartum from primiparous Plg-R$_{KT}^{+/+}$ **(D)** and Plg-R$_{KT}^{-/-}$ **(E)** female littermates and immunostained with rat anti-Plg-R$_{KT}$ mAb. Images were obtained with a Keyence BZ-X700 (magnification X 200). For the expanded area in panel D, (magnification X 400).
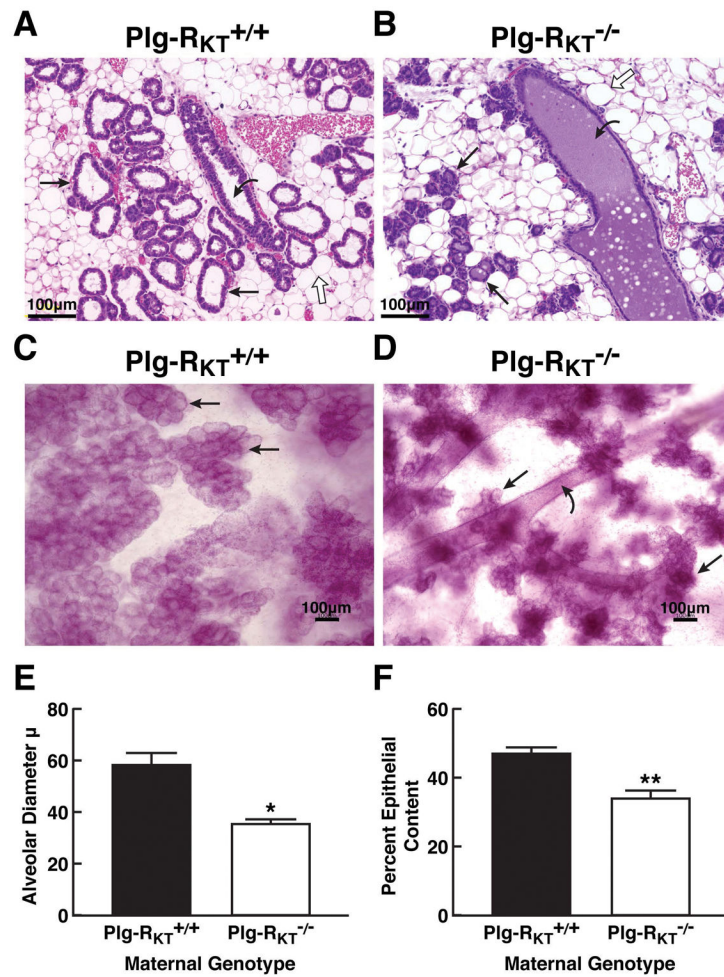
Figure 2. Blockade of lobuloalveolar development in Plg-R$_{KT}$ null mice

Histology of abdominal mammary glands of Plg-R$_{KT}$$^{+/+}$ mice **(A)** and Plg-R$_{KT}$$^{-/-}$ littermates **(B)** harvested 2 days postpartum and stained with H&E. Slides are representative of 6 mice from each group. Images were obtained with a Keyence BZ9000 (magnification X 200). Whole mounts of abdominal mammary glands from the same set of Plg-R$_{KT}$$^{+/+}$ mice **(C)** and Plg-R$_{KT}$$^{-/-}$ mice **(D)** harvested 2 days postpartum were prepared as described [39] and stained with carmine red. Images were obtained with a Keyence BZ-X700 (magnification X 100). Straight arrows indicate alveoli, curved arrows indicate ducts and open arrows indicate adipocytes. In Panel C, the visibility of ducts is blocked by the extensive alveoli present. **(E),** Alveolar diameters of abdominal mammary glands harvested 2 days postpartum. *P=0.01, n=5 Plg-R$_{KT}$$^{+/+}$ mice and n=3 Plg-R$_{KT}$$^{-/-}$ mice. **(F),** Per cent epithelial content of abdominal mammary glands harvested 2 days postpartum. *P=0.0011, n=6 Plg-R$_{KT}$$^{+/+}$ mice and n=3 Plg-R$_{KT}$$^{-/-}$ mice.
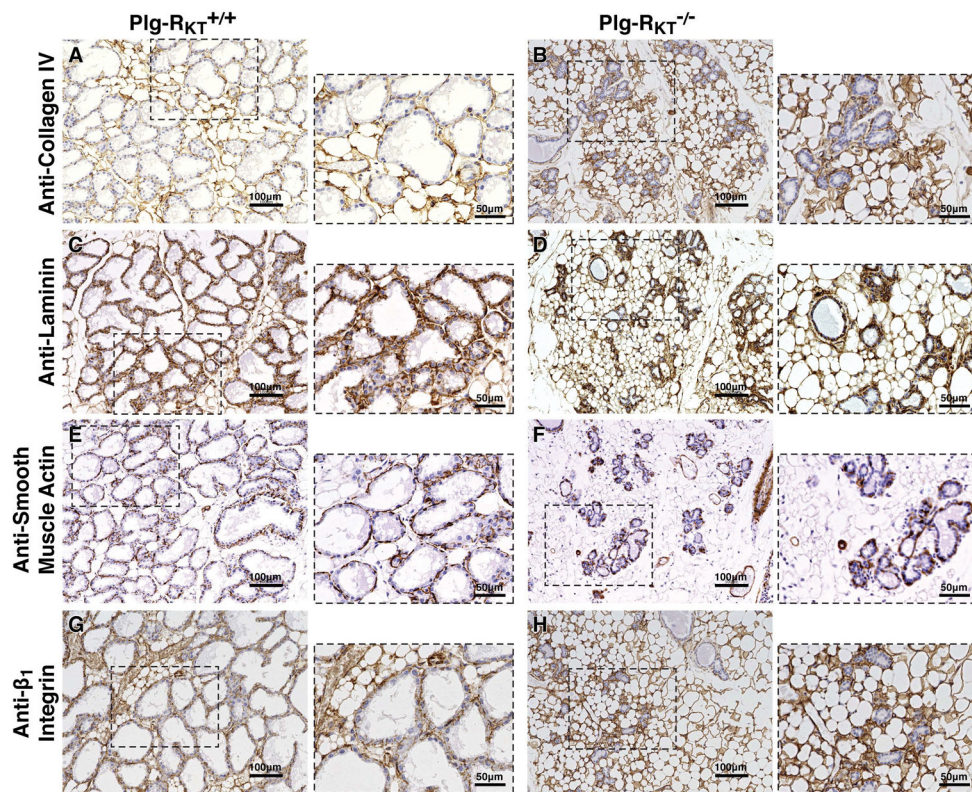
Figure 3. Plg-R_{KT} deletion does not affect basement membrane deposition of epithelial cells nor disrupt the myo-epithelial cell layer of mammary glands, but alters deposition of basement membrane components within the stroma

Abdominal mammary glands were harvested from Plg-R$_{KT}$$^{+/+}$ **(A,C,E,G)** and Plg-R$_{KT}$$^{-/-}$ **(B,D,F,H)** female mice two days postpartum and immunostained with antibodies against collagen IV **(A,B),** laminin **(C,D),** smooth muscle actin **(E,F)** or β$_1$-integrin **(G,H)**. Images were obtained with a Keyence BZ-X700 (magnification X 200). For the expanded areas, magnification X 400.
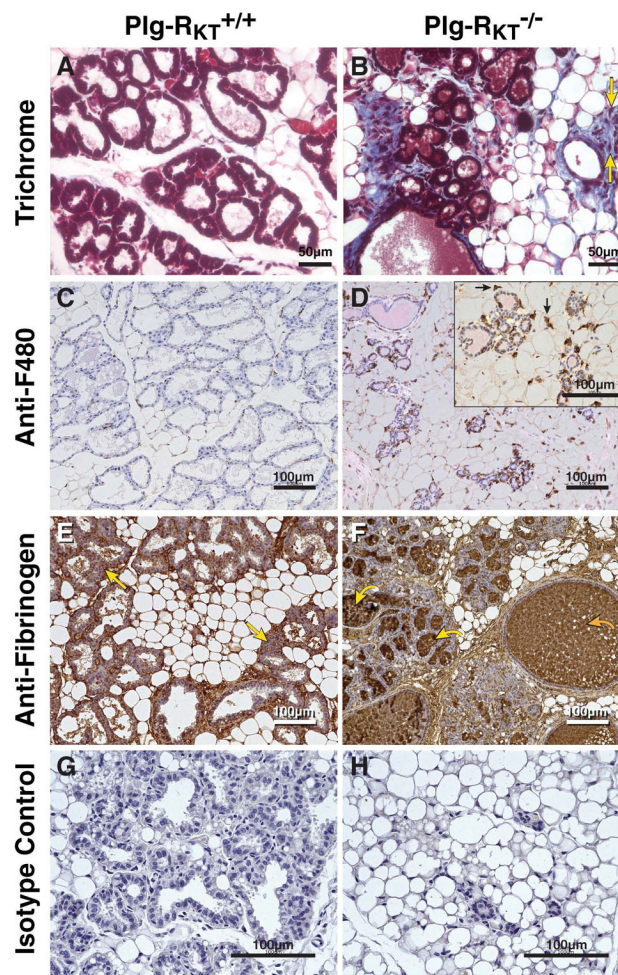
Figure 4. Plg-R$_{KT}$ deletion alters the ECM in lactating mammary glands

Abdominal mammary glands were harvested from Plg-R$_{KT}$$^{+/+}$ **(A,C,E,G)** and Plg-R$_{KT}$$^{-/-}$ **(B,D,F,H)** female mice two days following postpartum and stained with trichrome (blue) (yellow arrows label representative infiltrating cells) **(A,B)**, anti-F4/80 against macrophages (black arrows label representative macrophages) **(C,D)**, anti-fibrin(ogen) (the curved yellow arrow labels representative fibrin deposition in alveoli; the curved orange arrow labels representative fibrin deposition in dilated ducts; the straight yellow arrows labels representative fibrin deposition in adipose tissue) **(E,F),** or non-immune rabbit IgG control **(G,H)**. For A, B, G,H, images were obtained with a Keyence BZ9000 (magnification X 400). For C–F, Images were obtained with a Keyence BZ-X700 (A–H magnification X 200). For the inset in panel D, (magnification X 400).
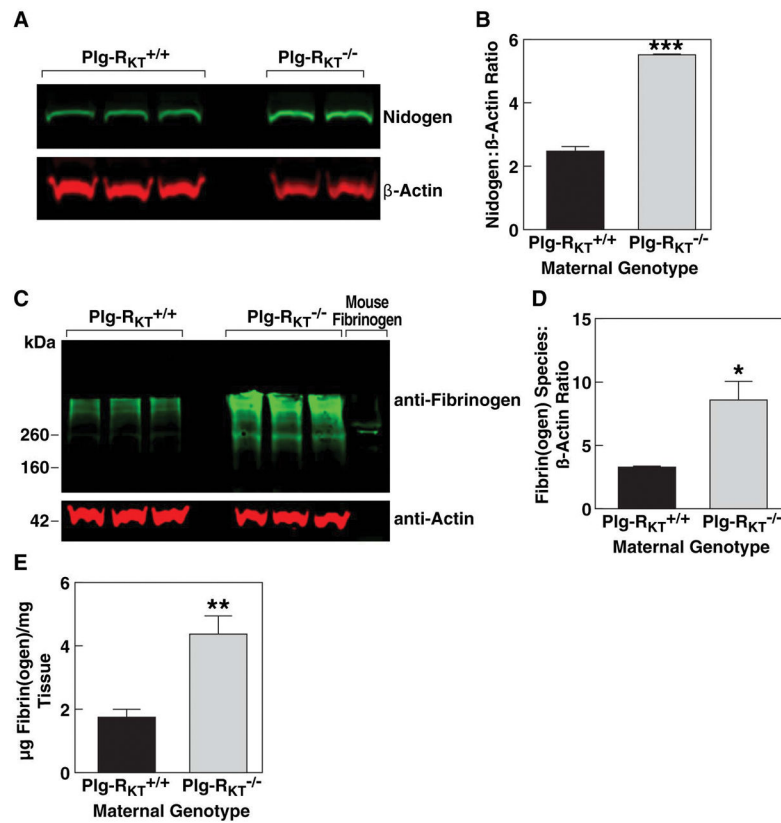
Figure 5. Decreased nidogen and increased fibrin content in Plg-R$_{KT}$$^{-/-}$ lactating mammary glands

Thoracic mammary glands were harvested from Plg-R$_{KT}$$^{+/+}$ and Plg-R$_{KT}$$^{-/-}$ female mice two days postpartum. Glands were lysed and electrophoresed on 4–12% gradient gels under reducing conditions and western blotted with anti-entactin/nidogen and anti-βactin **(A)** or electrophoresed under non-reducing conditions and western blotted with anti-fibrin(ogen) and anti-βactin. **(C).** Gels were scanned and quantified densitometrically using LI-COR software **(B** (***=P=0.0007, n=2–3) **D** (*=P=0.027, n=3). Total fibrin(ogen) content of glands was determined by ELISA **(E)** (**P=0.0016, n=8).
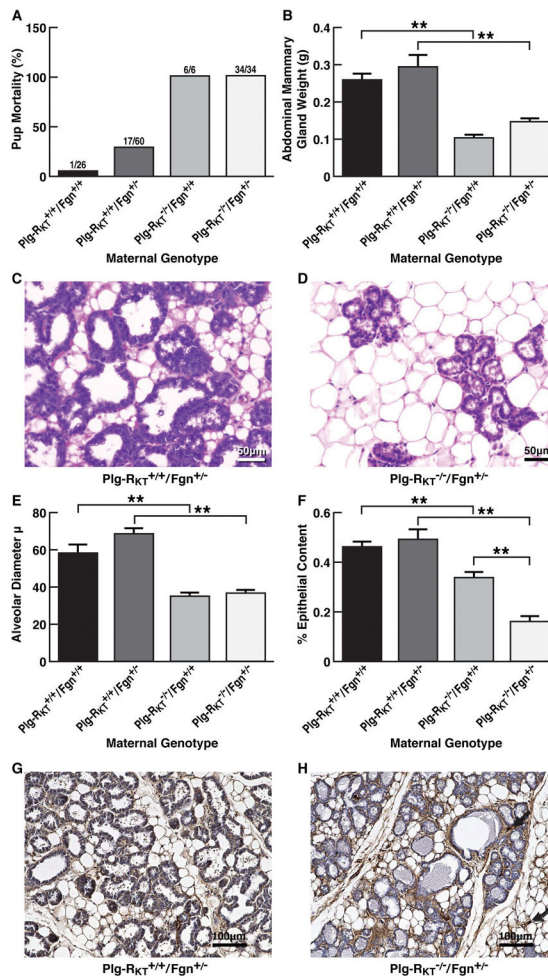
Figure 6. Effect of fibrinogen heterozygosity on alveolar development and lactational competence in Plg-R$_{KT}$$^{-/-}$ mice

(A), Pup mortality as a function of maternal genotype. **(B),** Abdominal mammary glands were collected 2 days postpartum from primiparous Plg-R$_{KT}$$^{+/+}$/Fgn$^{+/+}$, Plg-R$_{KT}$$^{+/+}$/Fgn$^{+/-}$, Plg-R$_{KT}$$^{-/-}$/Fgn$^{+/+}$ and Plg-R$_{KT}$$^{-/-}$/Fgn$^{+/-}$ female littermates and weighed. ANOVA revealed group differences: F=13.10, P,0.0001. **=p< 0.05 by Student-Newman-Keuls post hoc testing, n=6–12. Paraffin embedded Plg-R$_{KT}$$^{+/+}$/Fgn$^{+/-}$ glands **(C)** and Plg-R$_{KT}$$^{-/-}$/Fgn$^{+/-}$ glands **(D)** were stained with H&E. Images were obtained with a Keyence BZ9000 (magnification X 400). Slides are representative of 6 mice from each group. **(E)** Alveolar diameters of Plg-R$_{KT}$$^{+/+}$/Fgn$^{+/+}$, Plg-R$_{KT}$$^{+/+}$/Fgn$^{+/-}$, Plg-R$_{KT}$$^{-/-}$/Fgn$^{+/+}$ and Plg-R$_{KT}$$^{-/-}$/Fgn$^{+/-}$ glands harvested 2 days postpartum. ANOVA revealed group differences: F=23.90, P<0.001. **=p< 0.05 by Student-Newman-Keuls post hoc testing, n=6–12. **(F)** Per cent epithelial content of Plg-R$_{KT}$$^{+/+}$/Fgn$^{+/+}$, Plg-R$_{KT}$$^{+/+}$/Fgn$^{+/-}$, Plg-R$_{KT}$$^{-/-}$/Fgn$^{+/+}$ and Plg-R$_{KT}$$^{-/-}$/Fgn$^{+/-}$ glands harvested 2 days postpartum. ANOVA revealed group differences: F=18.79, P<0.001. **=p< 0.05 by Student-Newman-Keuls post hoc testing, n=6–12. Paraffin embedded Plg-R$_{KT}$$^{+/+}$/Fgn$^{+/-}$ **(G)** and Plg-R$_{KT}$$^{-/-}$/Fgn$^{+/-}$ **(H)** glands harvested 2 days postpartum were immunostained with anti-fibrinogen. Images were obtained with a Keyence BZ-X700 (magnification X 200). Curved arrow indicates fibrin deposition in

stroma surrounding the adipose tissue and straight arrow indicates fibrin deposition surrounding the alveoli.
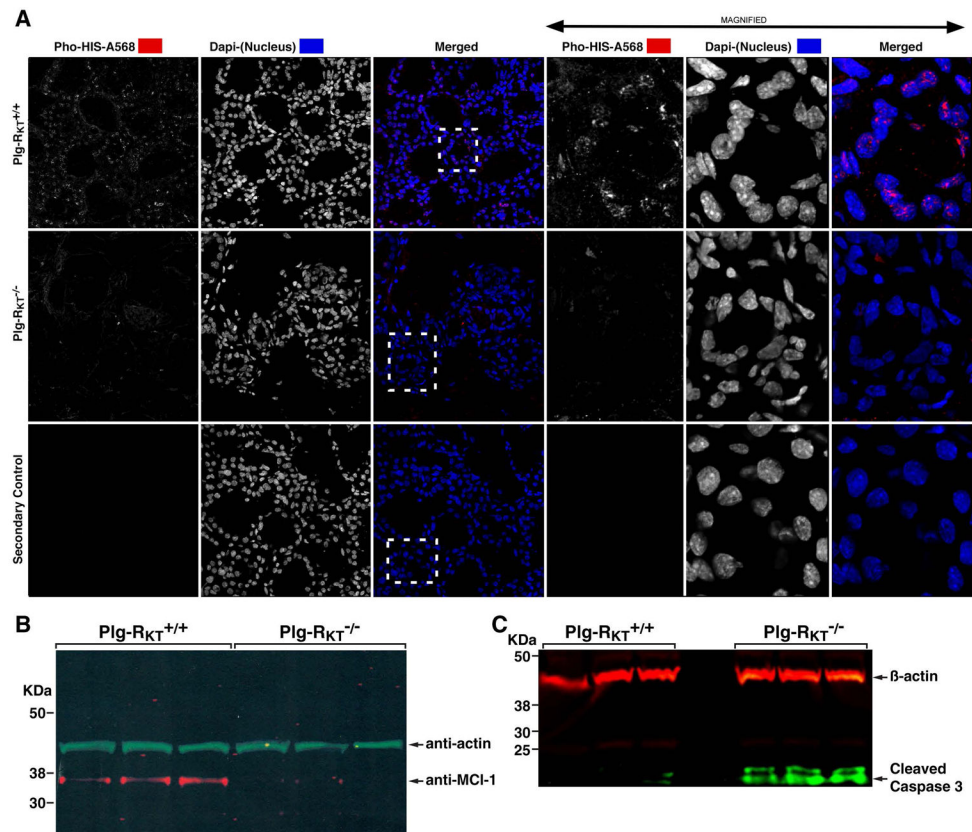
Figure 7. Plg-R$_{KT}$ deletion decreases epithelial cell proliferation and increases epithelial cell apoptosis

Mammary glands were harvested two days postpartum from Plg-R$_{KT}$$^{+/+}$ and Plg-R$_{KT}$$^{-/-}$ female mice. Frozen sections of abdominal mammary glands were immunostained with antibodies against Ser$_{28}$-phosphorylated histone H3 (Pho-HIS-A568) and Dapi (shown in white for greater clarity). Boxes defined by dashed lines are the areas enlarged in right panels. Confocal images were captured using a Zeiss 710 Laser Scanning Confocal Microscope running the Zen 2016 software. 8 bit optical image section slices (sampled at 0.3μm intervals) were collected as 1024×1024 images, converted to maximum intensity projections for 2D analysis then imported into: Image Pro Premier, Image J and LSM Examiner software for further processing and quantitative analysis. **(A).** Thoracic glands were lysed and electrophoresed on 4–12% gradient gels under reducing conditions and western blotted with anti-Mcl-1 and anti-βactin **(B)** or anti-active (cleaved) caspase 3 and anti-βactin **(C).**

Table 1

Genes Differentially Expressed in Lactating Mammary Glands of Plg-R$_{KT}$$^{-/-}$ Mice and Plg-R$_{KT}$$^{+/+}$ Mice

Gene Symbol	Description	Fold Regulation	P Value
Ctgf	Connective tissue growth factor	9.5461	0.000306
Edn1	Endothelin 1	4.7346	0.00814
Grem1	Gremlin 1	3.5022	0.040351
Hgf	Hepatocyte growth factor	6.1685	0.031379
Il1a	Interleukin 1 alpha	9.7242	0.025592
Il4	Interleukin 4	3.7884	0.029965
Itga2	Integrin alpha 2	15.7061	0.007263
Itgb1	Integrin beta 1 (fibronectin receptor beta)	2.4004	0.026171
Itgb3	Integrin beta 3	10.0788	0.018231
Itgb6	Integrin beta 6	3.9084	0.009638
Itgb8	Integrin beta 8	11.1573	0.015793
Ltbp1	Latent transforming growth factor beta binding protein 1	16.3164	0.004637
Mmp2	Matrix metallopeptidase 2	5.1512	0.02475
Mmp9	Matrix metallopeptidase 9	3.1057	0.027788
Pdgfb	Platelet derived growth factor, B polypeptide	2.5255	0.045256
Serpine1	Serine (or cysteine) peptidase inhibitor, clade E, member 1	3.2676	0.046089
Smad2	MAD homolog 2 (Drosophila)	2.2474	0.03523
Tgfb3	Transforming growth factor, beta 3	8.3682	0.006022
Tgfbr1	Transforming growth factor, beta receptor I	2.5726	0.044485
Timp2	Tissue inhibitor of metalloproteinase 2	6.5052	0.02108
Tnf	Tumor necrosis factor	5.2111	0.017668
Akt1	Thymoma viral proto-oncogene 1	−2.7993	0.00061
Egf	Epidermal growth factor	−12.2957	0.000286
Mmp1a	Matrix metallopeptidase 1a (interstitial collagenase)	−3.7496	0.002683
Timp4	Tissue inhibitor of metalloproteinase 4	−2.4511	0.013536

Regulated genes with Ct threshold < 35, P value <0.05 and > 2-fold change differences, n=3 per group